Near Wake Flow Field Measurements of a Marine Current Turbine: Preliminary Results

Ethan Lust[1], Luksa Luznik, Karen Flack, Julio Barros
Mechanical Engineering Department,
U.S. Naval Academy
Annapolis, MD, USA
[1]lust@usna.edu

***Abstract*—More advanced simulation tools are required to predict the loads experienced by a turbine in situ due to the surrounding environment including the effects of inflow turbulence, the impact of turbines operating upstream, the effect of the free surface, and the impact of surface waves, to name a few. These advanced models require detailed data sets for validation. At this time, few studies have focused on the near wake in an effort to provide such detailed data. It is critical to understand this region because it is where much of the high-energy phenomena occur that is most likely to impact turbine performance and reliability. To this end, a towing-tank particle image velocimetry (PIV) system was designed, built, and used to provide measurements of the flow in the near wake of a scale-independent marine current turbine. Included are preliminary results including a representative case and turbulent statistics for an ensemble of realizations.**

Keywords—marine current turbine; flow field; wake survey; towing tank; PIV

I. INTRODUCTION

The marine current turbine, like its more technologically mature contemporary, the wind turbine, produces power from an abundant source that is clean and sustainable making it attractive to those in search of alternative energy sources. Marine current turbines are superior to wind turbines with regard to specific power output (i.e. the swept area of the turbine per unit power produced, a consequence of the difference between the density of water and the density of air), and the predictability of marine currents. Despite these advantages there are, however, significant barriers to implementation. The marine operating environment is uncertain and unforgiving which translates into considerable expense to build, install, and maintain a marine current turbine. The development of high-fidelity models will help to reduce the uncertainty and help lower the barriers to wide-scale implementation.

In an effort to spur development of marine current turbine technology the U.S. National Renewable Energy Laboratory promulgated Reference Model 1 (RM1), shown in Fig. 1, and called for the development of computational models, studies describing the environmental impact, and the establishment of methods of life cycle cost estimation [1]. This paper focuses on the first of these goals, to provide experimental data, near-wake velocity profile data specifically, for model validation.

This study was sponsored by the Office of Naval Research

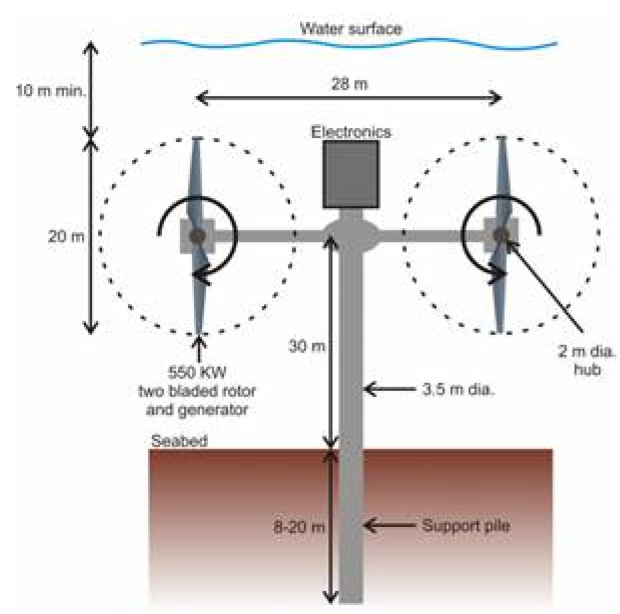

Fig. 1: Reference Model 1 (RM1) promulgated by the U.S. National Renewable Energy Laboratory [1].

Detailed wake measurements might also lead to a better understanding of the complex interactions between the inflow, the turbine, and the wake.

To date, a number of studies have been focused on mapping the wake of a horizontal axis marine current turbine using scale models of two- and three-bladed turbines including Neary, Gunawan, Hill, and Chamorro [2], Chamorro et al. [3], and Tedds, Owen, and Poole [4]. In their study, Neary, Gunawan, Hill, and Chamorro [2] used acoustic Doppler velocimetry (ADV) to characterize the streamwise velocity of a 1/10th scale, three-bladed axial flow turbine measuring D=0.5m, where D is the turbine diameter, in a water channel. The velocity measurements were taken at 1D upstream and 1, 3, 5, 9, and 15D downstream, and it was shown that the streamwise velocity recovered to approximately 80% of upstream levels by 10D indicating possible optimal array spacing of 10-15D. Chamorro et al. [3], using a similar experimental setup presented a number of new insights on the coupling between the turbine frequency and those observed in the wake. They also showed wake meandering, a phenomenon characteristic of wind turbines, noted for the first time in marine current turbine literature. Tedds, Owen, and Poole [4] investigated the near wake, defined as less than 7D from the rotor plane, for a three-bladed, horizontal-axis turbine measuring 0.5 m in diameter with a blade cross-section based on a NACA airfoil. They made observations both upstream and downstream of the turbine out to a distance of 7D. At each downstream location, spanwise measurements were taken at five different depths. Results demonstrated a high degree of anisotropy in the turbulence due to swirl effects, gradually decreasing but persistent well beyond 7D.

Several studies have focused specifically on near-wake phenomena including the velocity deficit, wake structure uniformity, wake rotation, coherent, persistent tip vortices, wake expansion, and hub vortices. These include Naumov et al. [5] who used stereo particle image velocimetry (SPIV) to examine the wake structure of a three-bladed model turbine measuring 0.376 m in diameter in a recirculating water channel. Conclusions included confirmation of theoretical predictions including the slowdown of the axial wake velocity, the absence of tangential rotation for tip vortices, and the confirmation of the far-wake model which assumes the wake structure to be uniform in the near wake (< 3*D*) and increasingly diffuse and incoherent in the far wake (> 3*D*).

Chamorro, Troolin, Lee, Arndt, and Sotiropoulos [6], in a study related to the two previously discussed, used Volumetric 3-component Velocimetry (V3V) to visualize the velocity field at three ranges downstream of the turbine: x/D = 0 to 1, 2 to 3, and 4 to 5. Instantaneous averaged and phase-averaged velocity fields were rendered showing wake expansion proportional to one-third power of the streamline distance. Strong coherent vortical structures were observed at $x/D < 1$ but became unstable for $x/D > 2$. Instability was hypothesized to come from the complex vortex interaction by which successive vortex rings catch up with and destructively interact with the next downstream vortex ring. Wake rotation was clearly visible, rotating in the opposite direction of turbine due to conservation of angular momentum, and shown to persist to a distance of $x/D \approx 3$. Hub vortices were also observed, but how they interact with tip vortices remains unclear.

The objectives of this work are to take detailed measurements of the wake of a scale-independent turbine under steady conditions in order to provide experimental validation for computational models. Steady results will be compared to those of a turbine in an unsteady flow field (i.e. in the presence of surface gravity waves) to determine the impact of waves on the wake.

II. Experimental Methods

A. Towing Tank

Experiments were conducted in the large towing tank at the U.S. Naval Academy which measures 116 m long, 7.9 m wide, and 4.9 m deep. All experimental and data acquisition equipment was mounted to a carriage which was towed for all experiments at 1.68 m/s.

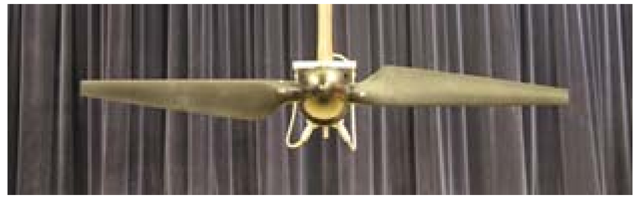

Fig. 2: The two-bladed horizontal axis marine current turbine used in the present experiment, shown mounted to the dynamometer with the data acquisition cables for thrust and torque protruding from below.

B. Model Turbine

The turbine used in this experiment, shown in Fig. 2, is a 1/25th scale, two-bladed horizontal-axis design measuring 0.8 m in diameter based on RM 1 (Fig. 1). The turbine diameter was selected to maximize the Reynolds number, as calculated using the $0.7R$ chord, where R is the blade radius, while remaining within dynamometer operating limitations. The blades are twisted from 13° at the root to 2° at the tip and tapered from a maximum chord length of 7 cm to a minimum of 2.5 cm.

The blades were mounted just aft of a nacelle measuring 8 cm in diameter and were manufactured at the U.S. Naval Academy using a 5-axis Computer Numerical Control milling machine from 6061 Aluminum, selected for its excellent machinability and corrosion resistance. The blades were given a matte black anodized finish to provide contrast for imaging experiments.

C. Experimental Apparatus

The equipment used to measure turbine performance parameters is shown in Fig. 3. Thrust and torque were measured using a Cussons R46 dynamometer, mounted in line with the turbine shaft. Shaft rotation speed and blade position were measured using a BEI Sensors H35 incremental optical encoder. The tip speed ratio was adjusted using a Placid Industries, Inc. H250 hysteresis brake attached to the output shaft. The brake also served to dissipate the power produced by the turbine. All instruments were synchronized in time. Performance parameter (i.e. carriage speed, shaft speed, torque and thrust) sampling was conducted at a rate of 700 Hz. Each run provided 30-40 s of steady state data at a carriage speed of 1.68 m/s with the brake set to provide a tip speed ratio (TSR) of approximately 7. The tip speed ratio is the rotation speed normalized by the free stream speed:

$$TSR = \frac{R\Omega}{U_\infty} \tag{1}$$

where Ω is the shaft speed, approximately 32 rad/s (5 rps), and U_∞ is the carriage speed, measuring 1.68 m/s (5.5 ft/s).

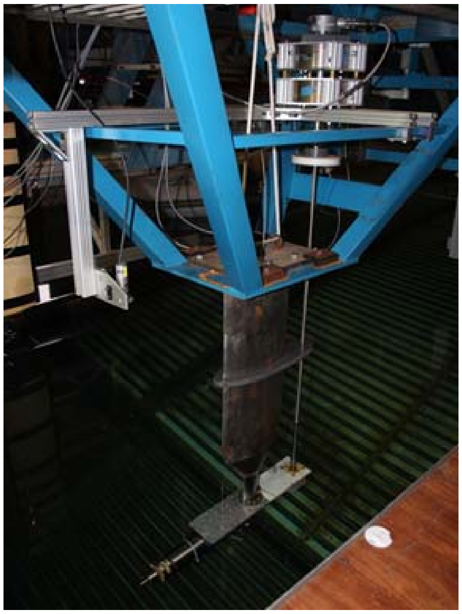

Fig. 3: Experimental apparatus including the shaft speed encoder, magnetic brakes, surface-piercing strut, and dynamometer (submerged, without the turbine installed).

A *TSR* of 7 was selected because it corresponds approximately to maximum power production, quantified by the power coefficient, C_P:

$$C_P = \frac{Q\Omega}{\frac{1}{2}\pi\rho U_\infty^3 R^2} \tag{2}$$

where Q is the torque, and ρ is the density of fresh water.

Quoted at 95% confidence using the Taylor Series Method described by the ISO/BIPM Guide for Uncertainty in Measurement (GUM) [7], over eight runs with constant experimental parameters the TSR was calculated to be 7.04 $\pm$ 3.8% and the resulting power coefficient was 0.43 $\pm$ 6.9%.

D. Towing Tank PIV System

To visualize the near wake of the turbine a 2-D Particle Image Velocimetry (PIV) system was designed and constructed to be fixed to the towing-tank carriage (Fig. 4). The system features two submersibles, one forward-looking and one side-looking. The laser or camera can be mounted in either submersible providing sub-surface visualization capability in planes parallel to both the long and short axes of the towing-tank.

The PIV system features a Quantel Evergreen, dual cavity, Nd:YAG 200 mJ 532 nm laser capable of a repetition rate of 15 Hz. The light sheet was formed using a 1000 mm spherical lens in combination with a 15 mm cylindrical lens. The camera is a TSI PowerView Plus 4MP CCD camera with a resolution of 2048 x 2048 pixels providing a nominal pixel width of 7.4 µm for a 30 cm by 30 cm field of view. A 50 mm lens was used with remote focus and aperture adjustment. The camera has a frame rate of 7.25 PIV image pairs per second (in Straddling Mode) and was positioned approximately 1.4 m from the light sheet.

Image pair capture was triggered by a Hall Effect sensor mounted to the turbine hub so as to phase lock the image pairs for a single run with the blades positioned horizontally. The seed particles used in this experiment were Potters Industries Sphericell® 110p8 hollow glass microspheres. The mean particle size was 12µm and a density ranged from 1.05-1.15e3 kg/m^3.

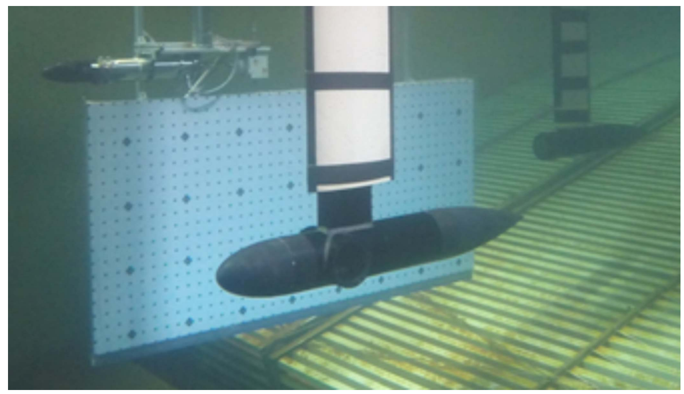

Fig. 4: An underwater view of the field of investigation including the dynamometer and turbine (turned so that the blades are horizontal), the target board (included in the image for reference but removed during data acquisition), the side-looking submersible which contained the camera, and the forward-looking submersible which contained the laser light arm and optics. During data acquisition, flow enters from the left.

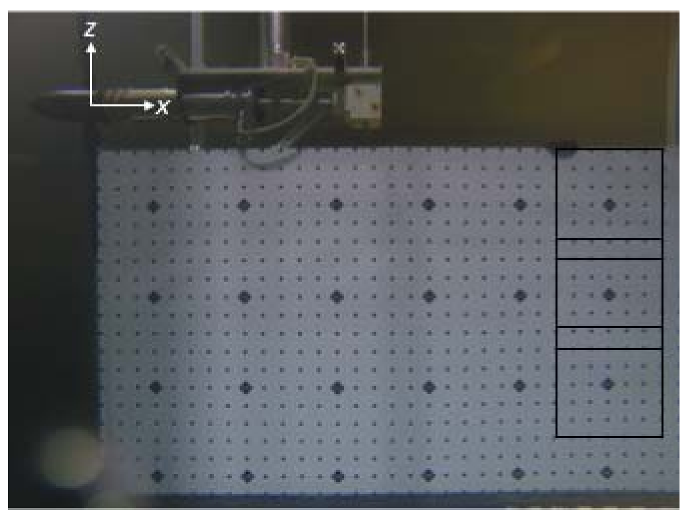

Fig. 5: An underwater view of the field of investigation. The squares encompass each of the three fields of view, each centered on the fiducial marker (solid diamond). Flow enters from the left.

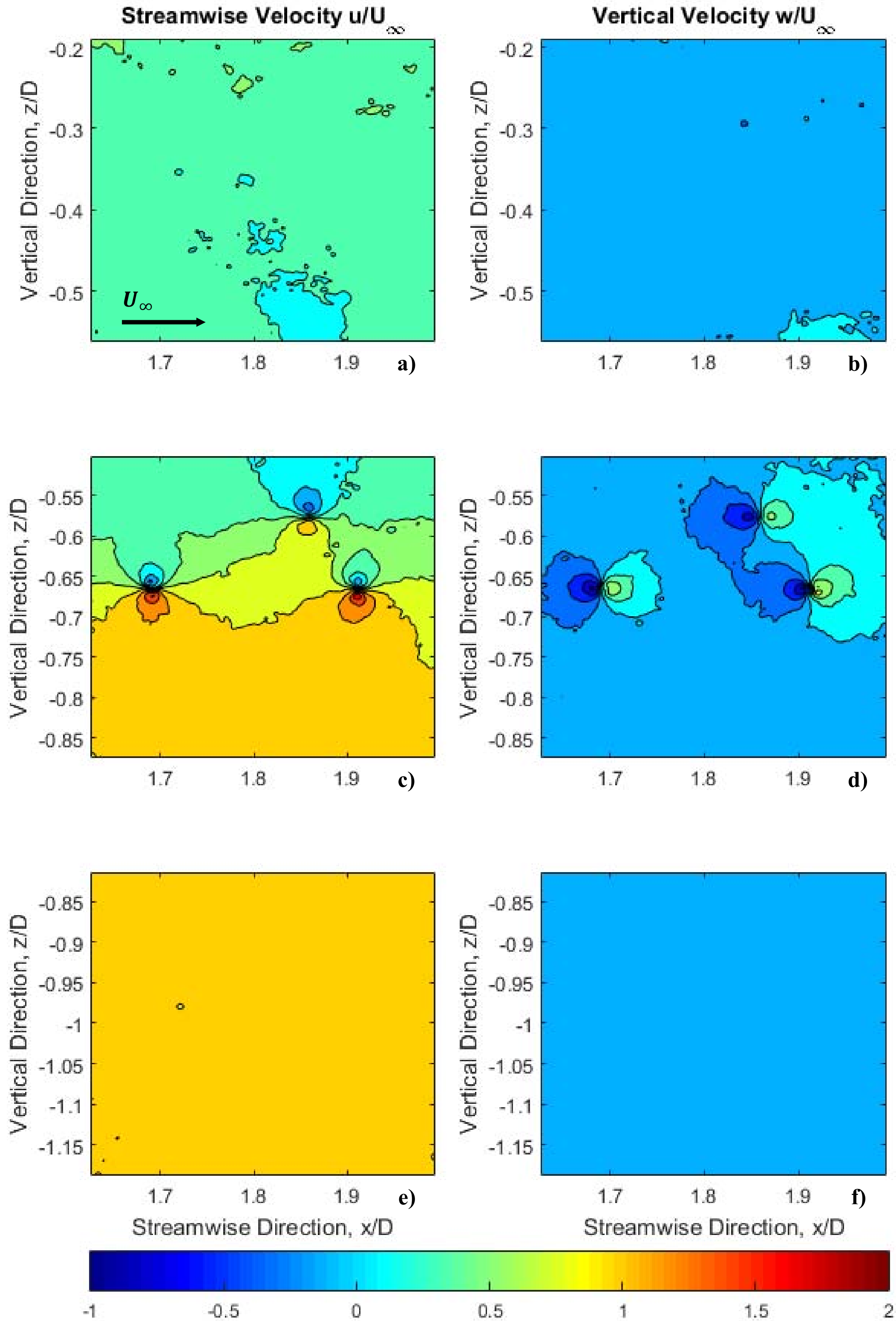

Fig. 6: The instantaneous velocity distribution in the streamwise direction (a, c, and e) and the vertical direction (b, d, and f) for each of the three vertically oriented positions. The mean flow is from left to right. The turbine would be located above and to the left of these positions and rotates clockwise when viewed from a position upstream of the turbine.

III. Preliminary Results

A. Data Acquisition Scheme

For the purposes of this discussion, the x-axis is defined as oriented parallel to the long axis of the towing tank with positive direction oriented downstream. The z-axis is defined as the vertical direction, with positive directed upward. The origin for position reference is the center of the turbine hub, at the same x-position as the turbine blades (shown in Fig. 5).

The turbine wake was mapped along the x-z plane (from approximately 20 cm (0.25D) upstream of the turbine tip path to 155 cm (1.9D) downstream and extending downward from beneath the turbine output shaft to a distance of 80 cm (1D). Each individual field of view measured approximately 30 cm by 30 cm with 5 cm overlap between adjacent fields.

This discussion is limited to results obtained from observing three fields of view, oriented vertically as shown in Fig. 5, at a distance of 145 cm (1.8D) from the turbine tip path and extending from 15 cm to 95 cm (0.2 to 1.2D) below the turbine output shaft. Each field of view is labeled by row and column, referenced to the upper left-hand corner of the target board. The three fields of view shown in Fig. 5 are the top row (i.e. row 1) and the two beneath it, rows 2 and 3, all from column 6. Column 6 was selected for this discussion because previous experimentation [8] has shown that it is likely to contain the most active turbulence and also show full development of wake expansion. Five runs (traverses of the carriage) were conducted for each field of view, with each run yielding approximately 200 image pairs for a total of 1,000 image pairs at each position.

B. PIV Settings and Statistics

PIV images were captured and processed using TSI Insight 4G software. The time delay between image pairs was set to 1,000 µs during which time the blades rotated 0.03 rad (1.7°). Camera exposure was set to 420 µs and the aperture and autofocus were not changed once set initially to ensure a consistent field of investigation.

At each position, 50 calibration images were taken and then averaged prior to calibration and de-warping yielding a pixel size of approximately 157 µm.

Images were processed using a recursive Nyquist grid engine (50% overlap), an FFT based correlation engine, where the sub-pixel displacement was estimated using a Gaussian peak engine. Vector validation was conducted using the local median filter and bad vector replacement was accomplished by valid secondary peaks from the local correlation maps. Any remaining holes were filled using local interpolation and the resulting vector fields were then low-pass filtered using a narrow Gaussian filter to remove high-frequency noise (higher than the spatial resolution).

The resulting particle displacements ranged from a minimum of approximately 2 px to a maximum of over 18 px, but the average displacement was approximately 8 px. Final interrogation spot size was set to 24 × 24 px providing a resolution of 12 px or 1.9 mm with less than 1% of vectors interpolated.

C. Results

Fig. 6 shows an instantaneous velocity field for three representative cases at each of the three vertically oriented positions described in Fig. 5. It should be noted that for each of the three positions (rows) the images were taken at approximately the same time during each respective run, but they are not simultaneous. The left-hand column (Fig. 6 a, c, and e) depicts the streamwise velocity, u and the right-hand column (Fig. 6 b, d, and f) depicts the vertical velocity, w. All position measurements are normalized by the blade diameter (0.8 m), and all velocity measurements are normalized by the free stream velocity which was 1.68 m/s $\pm$ 0.74% quoted at 95% confidence.

In the position closest to the turbine shaft (Fig. 6a), the velocity is approximately 40% of the free stream velocity at a horizontal distance of 2D downstream from the turbine tip path. No coherent structures are shown in this region, though the field of view is displaced from the output shaft by 15 cm (0.1875D) so there may be some phenomena not captured in the observation (e.g. hub vortices as shown in [6]). Vertical velocity variation in this position (Fig. 6b) is negligible.

The position shown in Fig. 6c and d is at the same depth as the turbine tip and clearly shows the tip vortices, which in this case are observed to meander even in the short distance of 2D. The shear layer between the wake and the mean flow is also clearly visible. The wake of a turbine has been observed by [6] and others to expand as a function of the horizontal distance from the turbine tip path to the 1/3 power. At a distance of 1.8D, the stream tube containing the wake should be approximately 0.6D from the turbine output shaft, which is corroborated by this observation.

At the furthest position from the turbine output shaft (Fig. 6e and f) the flow is shown to be at the free stream conditions.

The turbulent statistics depicted in Fig. 7 were calculated for a single position, the second row as shown in Fig. 6 which contains the tip vortices. Values were calculated using the ensemble of all the approximately 1,000 image pairs taken at that position over five runs.

Fig. 7a shows the turbulence intensity in the streamwise direction, I_u calculated

$$I_u = \frac{\sqrt{<u'^2>}}{U_\infty} \tag{3}$$

where u' is the fluctuating velocity in the streamwise direction. The transition from the turbulent wake in the vicinity of the tip vortices to the laminar flow outside the wake is clearly shown.

Fig. 7b, depicts the Reynolds Shear Stress, calculated

$$-\frac{\overline{< u'w' >}}{U_\infty} \tag{4}$$

A pair of tip vortices are clearly shown and despite the meandering indicated in Fig. 6 there appears to be a strong spatial coherence. The shear stress is shown to alternate sign from negative (blue) to positive (red) with the vortex rotating counterclockwise oriented as shown. Fig. 7c depicts the turbulence kinetic energy, calculated

$$k_{2-D} = \frac{< u'^2 + w'^2 >}{2U_\infty^2} \quad (5)$$

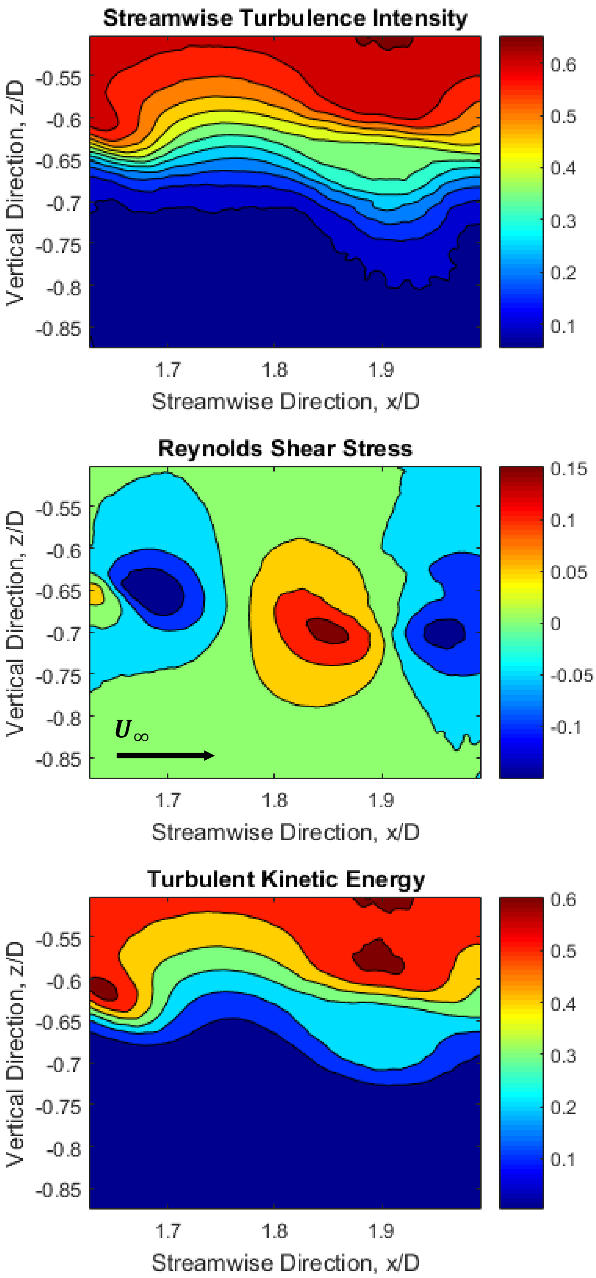

Fig. 7: The streamwise turbulence intensity (a), Reynolds shear stress (b), and turbulent kinetic energy (c) for the position enclosing the tip vortices (as shown in Fig. 6c and d). The mean flow is from left to right.

The turbulence kinetic energy is shown to peak in the same vertical plane as the vortices at or near the turbine tip. Again, the shear layer is clearly defined as the turbulence kinetic energy drops off rapidly outside the wake.

IV. Conclusions and Future Work

Preliminary results show many of the expected features of the turbine wake including a wake deficit of approximately 60% at 2D, wake expansion roughly following the 1/3 power law expansion, tip vortices, and a return to free-stream conditions outside the turbine stream tube.

The data presented in this discussion represent a small portion of the data taken during course of the experiment. Future work will include analysis of the entire field of investigation under steady conditions from 0.25D upstream of the turbine to 2.0D downstream, to a depth of 1.0D. The same experiment also included wake mapping in the presence of surface gravity waves. The steady flow field will be compared to the unsteady flow field to observe the impact of waves on turbine wake development.

Acknowledgment

The authors would like to thank the dedicated professionals of the U.S. Naval Academy's Technical Support Division, specifically Brandon Stanley and Mikael Koivula in the machine shop who fabricated the test apparatus, and John Zseleczky, Bill Beaver, and Dan Rhodes in the hydromechanics laboratory who helped to design and operate the system.

References

[1] R. Bagbey, R. Jepsen, R. Thresher, A. Copping, P. Mirko, Marine & Hydrokinetic Reference Model Development. [Presentation] 2011. Accessed June 15, 2013 http://www.globalmarinerenewable.com/images/stories/2011Presentations/IndustryDevelopmentDay/MHK_RM_Overview_2011_4-25.pdf.

[2] V.S. Neary, B. Gunawan, C. Hill, L.P. Chamorro, Near and far field flow disturbances induced by model hydrokinetic turbine: ADV and ADP comparison, Renewable Energy, vol. 60(0), pp. 1-6, 2013.

[3] L.P. Chamorro, C. Hill, S. Morton, C. Ellis, R.E.A. Arndt, and F. Sotiropoulos, On the interaction between a turbulent open channel flow and an axial-flow turbine, Journal of Fluid Mechanics, vol. 716, pp. 658-670, 2013.

[4] S.C. Tedds, I. Owen, R.J. and Poole, Near-wake characteristics of a model horizontal axis tidal stream turbine, Renewable Energy, vol. 63(0), pp. 222-235, 2014.

[5] I.V. Naumov, V.V. Rahmanov, V.L. Okulov, C.M. Velte, K.E. Meyer, and R.F. Mikkelsen, Flow diadnostics downtream of a tribladed rotor model, Thermophysics and Aeromechanics, 2012, vol. 19, no., 2, 2012.

[6] L.P. Chamorrow, D.R. Troolin, S. Lee, R.E.A. Arndt, F. Sotiropoulos, Three-dimensional flow visualization in the wake of a miniature axial-flow hydrokinetic turbine, Experiments in Fluids, vol. 54, no. 1459, January 2013.

[7] Evaluation of measurement data – guide to the expression of uncertainty in measurement, Joint Committee for Guides in Metrology, 2008. Accessed August 12, 2015: http://www.bipm.org/utils/common/documents/jcgm/JCGM_100_2008_E.pdf

[8] L. Luznik, M. Van Benthem, K.A. Flack, E.E. Lust, Near wake characteristics of a model horizontal axis marine current turbine under steady and unsteady flow conditions, Oceans - San Diego, 2013 , vol., no., pp.1,7, 23-27 Sept. 2013